Certification Report

Certified Reference Material

BAM-N008

Size distribution and concentration of

silver nanoparticles

calculated from small-angle X-ray scattering

(SAXS)

January 2023

Coordinator: A. F. Thünemann

Collaboration: K. Brademann, I. Breßler, M. Ebisch and P. Fengler

Bundesanstalt für Materialforschung und -prüfung (BAM)

Division 6.5 Synthesis and Scattering of Nanostructured Materials

Unter den Eichen 87

12205 Berlin, Germany

Phone: +49 30 8104 1610

E-mail: andreas.thuenemann@bam.de

Summary

This report describes preparation, analysis and certification of the silver nanoparticle reference material BAM-N008, including all analytical aspects and the proof of homogeneity and stability. Small-angle X-ray scattering (SAXS) was applied for characterization according to the international standard ISO 17867 [1]. Diameter and number density of the particles are provided as metrologically traceable values. Particle size distribution width and particle concentration are provided in not traceable form. The reference values for diameter, lognormal size distribution width, number density of particles and particle concentration are summarized in the table below.

Property	Value[1]	U[2]	Traceable[3]	Unit
Diameter[4] (D)	5.8	0.5 (9%)	yes	nm
Size distribution width[5] (σ)	1.33	0.18 (14%)	no	nm
Number density[6] (N)	3.7	0.7 (19%)	no	10^{-6} mol l^{-1}
Concentration[7] (c)	3.0	0.5 (17%)	no	g l^{-1}

1. Values are means from values of homogeneity study.
2. Expanded uncertainties $U = ku_c$ were calculated according to ISO Guide 35 [2] with the coverage factor $k = 2$ giving a level of confidence of approximately 95%. The value of the combined standard uncertainty u_c of the property includes an uncertainty contribution resulting from the study of homogeneity, long-term stability of the material, variation in the measurement results from a gold standard, and variation in the individual instruments.
3. Certified is labelled with "yes" for certified values, i.e., values are traceable to SI under the assumptions of the model used for interpretation of the SAXS data. Traceable is labelled as "no" for values without proven traceability.
4. Median value of the distribution of the diameters of the particles (for calculation, see Section 5.2.1).
5. Standard deviation of the width of the diameter size distribution (Section 5.2.1).
6. Number of particles per volume (Section 5.2.2)
7. Weight concentration (Section 5.2.3)

This report contains detailed information on the preparation of the reference material, as well as on homogeneity investigations and on the analytical methods used for certification analysis. The values are based on the results of homogeneity study. An example of a bottle of BAM-N008 containing a volume of 5 ml of aqueous dispersion of silver nanoparticles is shown in Figure 1.

Figure 1: Bottle of the reference material BAM-N008 containing a volume of 5 ml of aqueous dispersion of silver nanoparticles.

Contents

List of abbreviations

(if not explained elsewhere)

CRM	certified reference material
df	degrees of freedom
E_n	"normalized error", a measure of data compatibility
F	Fisher statistic
F_{crit}	critical value of the Fisher distribution
M	mean square
$M_{between}$	mean square between groups
M_{within}	mean square within group
MS	mean squared error
N	number of bottles
n	number of replicate determinations
NIST	National Institute of Standards and Technology
p	p-value
PTB	Physikalisch Technische Bundesanstalt
SAXS	small angle X-ray scattering
SS	sum of squares
s	standard deviation
s_{bb}	between-unit standard deviation
s_r	repeatability standard deviation
SRM	Standard Reference Material (NIST)
u_{bb}	uncertainty caused by inhomogeneity
u_{bias}	uncertainty caused by bias
u_{lts}	uncertainty caused by instability
u_{rep}	uncertainty caused by repeatability

1 Introduction

Nanoparticles reveal typically distinct changes of physical and chemical properties in comparison to the bulk material making them technologically attractive. The main reasons can be seen here in the small size and exceptionally large surface to volume ratio with a high fraction of atoms on the particles-to-surroundings interface. This led to a wide range of applications of nanomaterials, e.g., for hydrogen economy [3], but is accompanied by concerns on how save nanomaterials are [4]. Small silver particles are antibacterial and therefore, colloidal silver is used in medicine for a long time and their application is constantly being expanded [5]. Today there are hundreds of products available containing silver in form of nanoparticles, so-called nano silver. This situation and the foreseeable future growing market of nano silver will supposedly cause an increasing release of silver into the environment [6]. In this way, silver can be also incorporated into the human body and accumulated in different organs, which can be toxic or at least an unknown risk for the human health [7, 8, 9]. For these reasons, it is important to constantly study materials containing silver nanoparticles, their production, application in products and technical processes, dissemination of silver nanoparticles in the environment as well as effects to humans and the nature [10]. The state-of-the-art on characterization of nanoparticle size and concentration is illustrated in an extensive recent interlaboratory comparison [11]. To guarantee the traceability of measurements and to secure the comparison of results of different analytical methods, reference materials (RM) and certified reference materials (CRM) are essential [12]. The objective of this project is to provide an aqueous suspension of silver nanoparticles as reference material with a nominal diameter below 10 nm for application in determination of the size and concentration of nanoparticles in an aqueous surrounding. Measurands are the particles' diameter D, size distribution width σ, number density N and concentration c. Target uncertainties, defined as one sigma of the measurand values, are 5% for D, 10% for σ, 20% for N and 20% for c. The certification was carried out on the basis of ISO 17867 [1] and the relevant ISO-Guides for the production of reference materials [13, 14].

2 Material

2.1 Synthesis of silver nanoparticles

Starting materials. Water used for all preparations was MilliQ grade (18.2 MΩ at 25°C). All chemicals were used as received and without further purification. Silver nitrate was purchased from AppliChem, ethylene glycol from Acros. Poly(acrylic acid) was purchased from Fluka (catalog number 323667-250g).

Synthesis. The polyol process for silver nanoparticle synthesis was adapted from Hu et al. [15] and is described in detail elsewhere [16]. Briefly, solution 1 was prepared by solving 1.944 g (11.444 mmol) of silver nitrate under

stirring in 58.5 ml ethylene glycol at room temperature. Solution 2 was prepared by adding 15.7 g (217.9 mmol with respect to the monomer units) of poly(acrylic acid) to 291.5 ml ethylene glycol and heating the mixture under stirring to 200 °C. A short chain poly(acrylic acid) (PAA) with a molar mass of M_w = 1800 g mol^{-1} was chosen, which contains 25 monomer units per polymer chain. The ratio of silver ions to acrylic acid monomer units was 1 to 19. The solution 1 was added within 3 s to the boiling solution 2 under rigorous stirring. The mixture was boiled for 15 minutes and was then cooled down to room temperature. The processing of the particles started by adding 800 ml of water with a pH value of 5 and storing of the mixture for 24 h. Then the reddish-brown colored supernatant was decanted. This procedure was repeated three times. Then, the residue was suspended with 150 ml water. A 1% (w/v) sodium hydroxide solution was added in drops until the pH of the dispersion was adjusted to 10. The color turned from starting with reddish brown, via olive-green to brownish black. The amount of PAA in the final dispersion was 13% (w/w) related to the dry mass, as determined with thermogravimetric analysis (TGA) measurements. It should be noted that the samples were dried at 80 °C before TGA measurement to remove the water. An amount of 0.35 g PAA was added per liter suspension. This results in a final PAA amount of 30% (w/w) related to the dry mass, as confirmed with TGA. A total number of 19 batches according to the upper procedure was synthesized from May to August 2016 at BAM. All batches were mixed in a brownish colored flask with a volume of 10 liters to get a final volume of 7 liters of dispersion. This stock solution of candidate material was stored at a temperature of 20 ± 3 °C.

2.2 Preparation of the candidate material

The original stock solution has an approximate silver concentration of 3 g/l. The suspension was filled into brown plastic bottles of 5 ml content each using a bottle-top dispenser (Dispensette® III; type: Dig. Easy calibration 1-10 ml). The batch size of the lot is 1000 bottles. The used bottles are 8 ml HDPE Thermo Scientific Nalgene™ quality amber narrow-mouth bottles. This material reduces UV-light transmissions to protect light-sensitive liquids. The material of the bottles has an excellent chemical resistance to most acids, bases and alcohols. It is reliable and durable for long-term use. The used closures are normal leak-proof screw caps. These bottles are especially useful for long-term storage, shipping and packaging of liquids. The pH value of the suspension has been monitored. Although not critical, at the time of delivery the suspension has a pH value of around 10. An example of a filled bottle is shown in Figure 1.

3 Homogeneity

Twenty bottles have been selected randomly from the whole set of 1000 bottles. On three consecutive days, one sample per day was taken from each of the selected bottles and immediately measured with SAXS. To the best

of our knowledge, we can assume that the properties of the samples (changes after opening) and the framework conditions of the measurements (e.g. person performing the measurements) were the same on all 3 days. The resulting SAXS data curves were analyzed according to model fitting described in ISO 17867 [1] employing the model of homogeneous spheres with lognormal size distribution (details are provided in clause 5.2). The model fitting provides 60 values (one value for each bottle and every day) for each of the four measurands. An overview of the 20 samples on means and standard deviations of particle diameter D, diameter distribution width σ, particle number density N and concentration c is provided in Figure 2 (black circles and error bars). The overall means of the properties are D = (5.83 ± 0.13) nm, σ = (1.33 ± 0.05) nm, N = (3.74 ± 0.15) 10^{-6} mol l^{-1} and c = (3.04 ± 0.04) g l^{-1} (red squares and error bars represent the mean and one standard deviation of the mean, blue circles and error bars indicated the mean and two standard deviations).

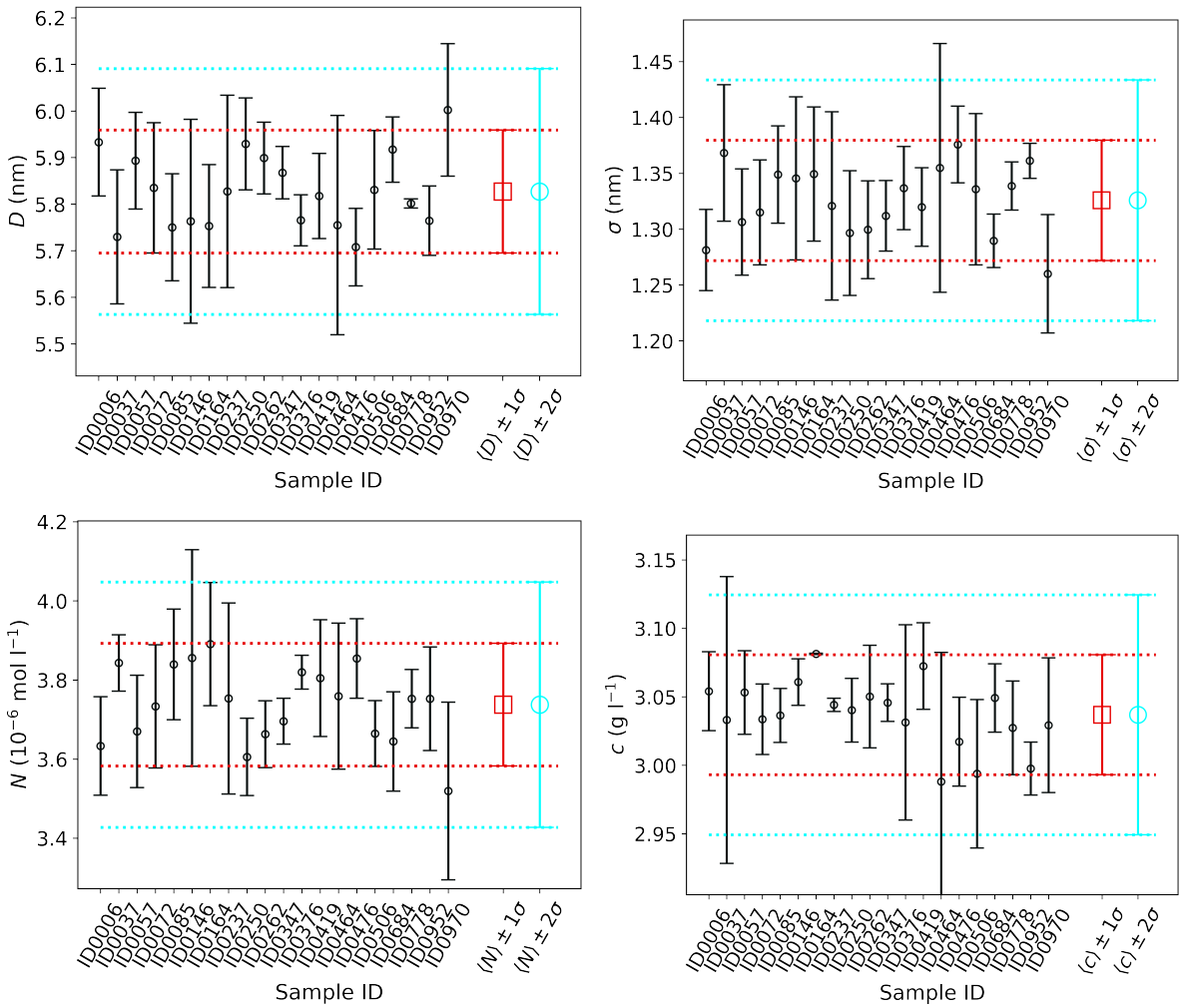

Figure 2: Homogeneity study on the diameter D, size distribution width σ, particle number density N and particle concentration c. The 20 samples of the study are indicated by their sample IDs. Black circles and error bars represent the mean value and the standard deviation for the property of each sample. Red squares and red error bars represent the overall mean and one standard deviation of the overall mean. Blue circles and error bars represent the overall mean and two standard deviations.

An analysis of variance (ANOVA) was performed for these measurands according to ISO Guide 35 [2]. Therein, the scattering of the values are expressed by the between-group ($M_{between}$) and within-group mean squares (M_{within}). These values were used for estimation of the standard uncertainties associated with between-bottle standard deviation as

$$s_{bb} = \sqrt{\max\left(\frac{M_{between} - M_{within}}{n_0},\ 0\right)} \tag{1}$$

where n_0 is the number of observations per group (here $n_0 = 3$; observation at days 1, 2 and 3). The s_{bb} is 0 if $M_{between} < M_{within}$. Further, the repeatability standard deviation is calculated as

$$s_r = \sqrt{M_{within}} \tag{2}$$

The between bottle and repeatability standard deviations are $s_{bb} =$ 0.034 nm and $s_r =$ 0.128 nm for D, $s_{bb} =$ 0 and $s_r =$ 0.054 nm for σ, $s_{bb} =$ 0.052 × 10^{-6} mol l^{-1} and $s_r =$ 0.146 × 10^{-6} mol l^{-1} for N and finally $s_{bb} =$ 0 and $s_r =$ 0.045 g l^{-1} for c. Results are summarized in the ANOVA Tables 1 to 4. The finding that the s_{bb}-values are very small or even 0 strongly indicates the absence of any between-bottle effect for D, σ, N and c. Such could have been expected because all bottles were filled from the same stock suspension and the nanoparticles are too small to sediment. ANOVA uses a variance-based F-test to test the group mean equality. Therein, the null hypothesis that all group means are equal cannot be rejected if the calculated F-value is below a tabulated critical value F_{crit}. Comparison of the data in Tables 1 to 4 shows that the F-value is always $< F_{crit}$, indicating that the group means are equal. The p-values, which are inversely related to the F-values, are additionally given in the Tables 1 to 4 as indicator for significance. The p-values of 0.298 (D), 0.498 (σ), 0.189 (N) and 0.595 (c) are much larger as the typically utilized threshold value of 0.05. Therefore, the p-values are not significant, and it can be concluded that the groups have equal variances.

To summarize, no evidence suggesting a rejection of the hypothesis that the material is sufficiently homogeneous was observed. In this case, the between unit homogeneity contribution to the uncertainty is identical to the between unit standard deviation, i.e.,

$$u_{bb} = s_{bb} \tag{3}$$

All data from the homogeneity study were accepted and pooled. Thus, total mean values for the four measurands and estimates of the uncertainty u_{bb} due to possible (undetected) inhomogeneity have been derived from the homogeneity study. Next, the repeatability standard deviations were utilized as estimates of the uncertainty of the repeatability of a single measurement, i.e.,

$$u_{rep} = s_r \tag{4}$$

Table 1: ANOVA table for between-bottle homogeneity study of D

Overall Mean (nm)	Overall s (nm)	Source of variation	SS	df	MS	s	F	F_{crit}	p-value
5.827	0.132	Between bottles	0.374	19	0.02	0.034	1.21	1.853	0.298
		Within bottles	0.65	40	0.016	0.128			
		Total	1.024	59					

Table 2: ANOVA table for between-bottle homogeneity study of σ

Overall Mean (nm)	Overall s (nm)	Source of variation	SS	df	MS	s	F	F_{crit}	p-value
1.326	0.054	Between bottles	0.055	19	0.003	0.0	0.983	1.853	0.498
		Within bottles	0.117	40	0.003	0.054			
		Total	0.171	59					

Table 3: ANOVA table for between-bottle homogeneity study of N

Overall Mean (10^{-6}mol l^{-1})	Overall s (10^{-6}mol l^{-1})	Source of variation	SS	df	MS	s	F	F_{crit}	p-value
3.738	0.155	Between bottles	0.56	19	0.029	0.052	1.386	1.853	0.189
		Within bottles	0.851	40	0.021	0.146			
		Total	1.411	59					

Table 4: ANOVA table for between-bottle homogeneity study of c

Overall Mean (g l^{-1})	Overall s (g l^{-1})	Source of variation	SS	df	MS	s	F	F_{crit}	p-value
3.037	0.044	Between bottles	0.034	19	0.002	0.0	0.891	1.853	0.595
		Within bottles	0.08	40	0.002	0.045			
		Total	0.113	59					

4 Stability

4.1 Short-term stability

The robustness of the material against external influences was tested for five randomly selected samples. Of interest were temperature and transportation stability. The sensitivity of the material against changes of the temperature was investigated first. For this purpose, one sample was frozen to -40°C, a second sample was cooled to 4°C and a third sample was heated to 70°C, each for 7 days. The remaining two samples were shipped in luggage, each for two ten-hour intercontinental flights. These five samples were measured with SAXS after temperature-treatment and transport, respectively. An overview on the results is given in Figure 3 (black circles). The means of the measurands from the homogeneity study are also plotted for comparison (red squares represent the means and the red error bars one standard deviation, blue error bars are two standard deviations). It can be seen that one value for D, σ and N and two values for c lie outside the interval of two standard deviations of the values of the homogeneity study (horizontal dashed blue lines). This indicates the presence of small but significant changes of the materials' properties by the applied external influences. Therefore, transportation times should be at the possible minimum. Additionally, exposure to lower and higher temperatures than 20 ± 3 °C should be avoided.

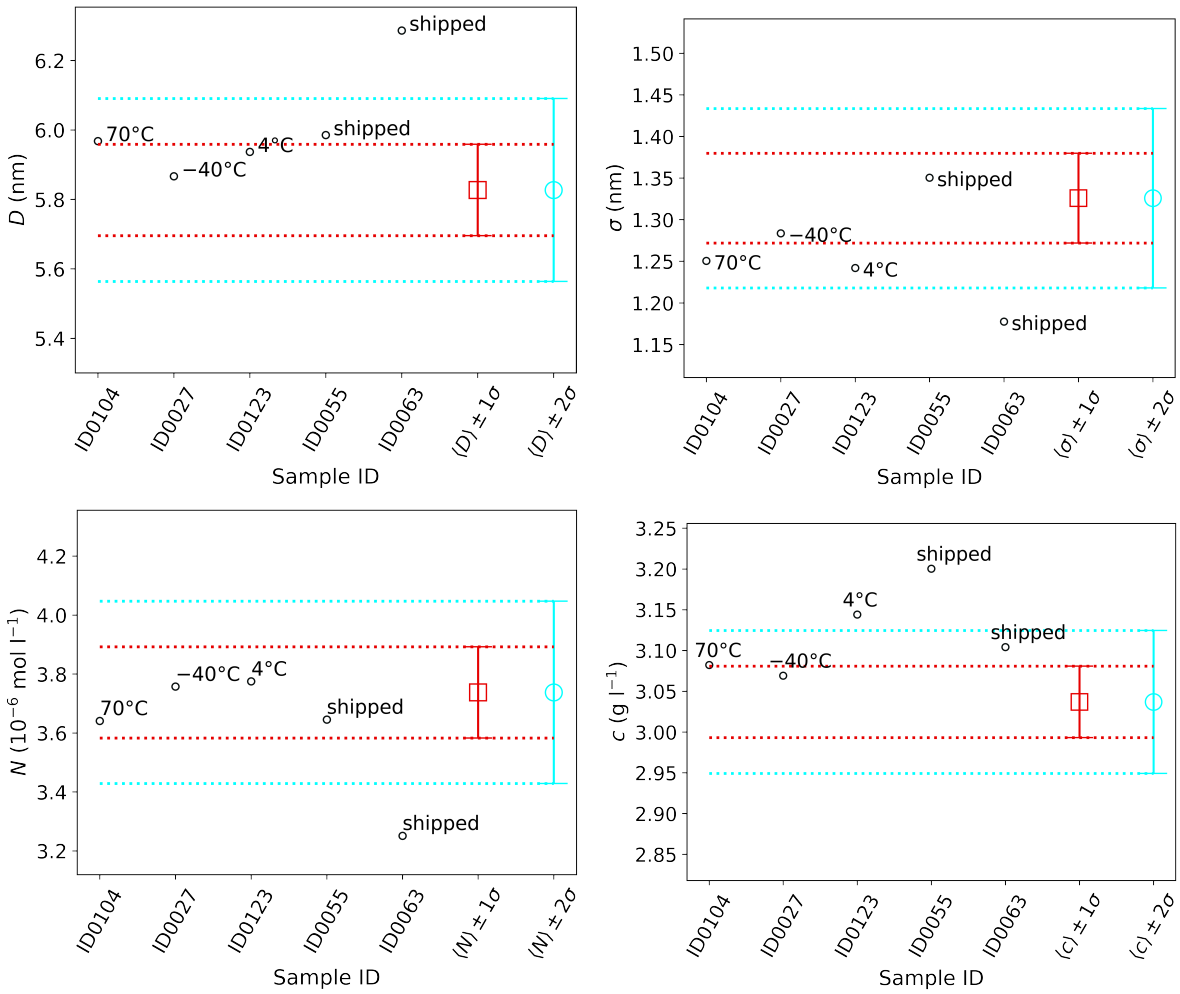

Figure 3: Short-term stability study on diameter D, size distribution width σ, particle number density N and particle concentration c. Conditions of the stability tests are given together with the data points (black circles). Red squares represent the overall means from the homogeneity study, and the red error bars are the corresponding standard deviation from the homogeneity study. Blue error bars are two standard deviations.

4.2 Long-term stability

A long-term stability study was performed after it was verified that the changes of the parameters due to variation of temperature and transport were significantly lower than defined by the target uncertainties (see clause 4.1). Start time ($t = 0$) of the study was the first day of the homogeneity study which was performed 354, 355 and 356 days after bottling of the samples. The reason for the long period between filling and the start of the homogeneity study was to find out whether the probability of long-term colloidal stability is high enough for the development of a reference material. The long-term stability study was conducted with 30 randomly selected bottles over a period of four years to access the materials' stability under the storage conditions specified for their lifetime, i.e., storage in the dark at an ambient temperature of (20 ± 3)°C. One of the 30 samples mentioned above was always selected at random for measurement. It should be noted that the measurements were always carried out when free measurement time was available, and not for reasons of optimizing the statistics. The overall means of the resultant measurand values are D = (5.82 ± 0.14) nm, σ = (1.34 ± 0.05) nm, N = (3.77 ± 0.19) 10^{-6} mol l^{-1} and c = (3.07 ± 0.05) g l^{-1}. An overview of the values of the measurands as a function of time of the study together with the means and their uncertainties is provided in Figure 4 (black spheres, horizontal red lines correspond to the mean, red and blue error bars represent one and two times the standard error of the values). Visible inspection shows that most values are within the target uncertainties of 5% (D), 10% (σ), 20% (N) and 20% (c) and all values are within two times of the target uncertainties (green dotted and green solid lines in Figure 4, respectively). For analysis of the presence of a time-dependent trend, the rate of changes of the parameters was estimated by a univariate linear model in accordance with clause B.3 of ISO Guide 35 [2]. Therein, the individual values of a measurand, y_i, are related to the time of measurement, x_i, by

$$y_i = b_0 + b_1 x_i \tag{5}$$

where b_0 and b_1 are the estimated intercept and slope, respectively. The regression parameters were calculated as

$$b_1 = \frac{\sum_{i=1}^{n}(x_i - \bar{x})(y_i - \bar{y}))}{\sum_{i=1}^{n}(x_i - \bar{x})^2} \tag{6}$$

and

$$b_0 = \bar{y} - b_1 \bar{x} \tag{7}$$

where $\bar{x}$ and $\bar{y}$ are the mean of the respective observations. The standard errors of b_1 and b_0 were calculated as

$$s(b_1) = s\left(\sum_{i=1}^{n}(x_i - \bar{x})^2\right)^{-1/2} \tag{8}$$

where

$$s^2 = \frac{1}{n-2} \sum_{i=1}^{n} (y_i - b_0 - b_1 x_i)^2 \tag{9}$$

and

$$s(b_0) = s(b_1) \left(\frac{1}{n} \sum_{i=1}^{n} x_i^2 \right)^{1/2} \tag{10}$$

The regression parameters from application of eqs. (6) and (7) were inserted in eq. (5) and the resulting linear regression lines are plotted in Figure 4 for a period of eight years (black solid lines). It can be seen that the slope is negative for D and positive for σ, N and c, i.e., the values decrease or increase with time. Next, the statistical significance of this finding was investigated according to clause B.3.4 [2]. Therein, the t-test is described for testing whether the b_1 differs significantly from zero. The t-statistics is calculated as

$$t_{b_1} = \frac{|b_1|}{s(b_1)} \tag{11}$$

The t_{b_1} is compared with the two-tailed critical value, $t_{95,n-2}$, of Student's t for $n-2$ degrees of freedom at the 95% level of confidence. Here, for $n = 78$ the $t_{95,n-2}$ is 1.99. The t_{b_1}-values are 1.15 (D), 5.86 (σ), 3.50 (N) and 12.16 (c). The t_{b_1}-value of D is smaller than t_c, i.e. the change of the particles' diameter is not significant. Since the t_{b_1}-values of σ N and c are larger than t_c, the slopes of the values of these measurands are considered to be significant. Consequently, the change of the measurand values over time has to be taken into account. The fitted values b_0 and b_1 were therefore used to provide an estimate $\hat{y}$ of the value of the response for a particular value $\hat{x}$, using

$$\hat{y} = b_0 + b_1 \hat{x} \tag{12}$$

The two-sided confidence interval at the 95% level of confidence is given by

$$\hat{y}_{\pm} = \hat{y} \pm t_{95,n-2}\ s \left(\frac{1}{n} + \frac{(\hat{x} - \bar{x})^2}{\sum_{i=1}^{n} (x_i - \bar{x})^2} \right)^{-1/2} \tag{13}$$

Regression lines according to eq. (12) and the confidence intervals for the regression lines derived from eq. (13) are shown in Figure 4 (black solid and black dashed lines). When accepting tentatively the model of a linear trend of the increase in the values, an extrapolation is possible to predict the storage lifetime (also called shelf-life). Alternatively, the interpolation is helpful to set a first monitoring point at which the validity of the measurand values needs to be checked.

The upper and lower limits of an acceptable range of values for a measurand of BAM-N008 can be defined as L_{upr} and L_{lwr}, respectively. The confidence interval around a predicting future value of a measurand is given by eqs. (12) and (13) when the degradation follows a simple linear form and taking $\hat{x}$ as the time from the beginning of the stability study. The required shelf-life is obtained by setting eq. (13) to each of the specification limits and

solving for $\hat{x}$ to obtain the shortest positive shelf-life t_{shelf} according to

$$t_{shelf} = \min\left(t_{s,upr}, t_{s,lwr}\right) \tag{14}$$

The times $t_{s,upr}$ and $t_{s,lwr}$ are the lowest positive solution to

$$L_{upr} = \left[b_0 + b_1 t_{s,upr} \pm t_{95,n-2}\, s\sqrt{\frac{1}{n} + \frac{(t_{s,upr} - \bar{x})^2}{\sum_{i=1}^{n}(x_i - \bar{x})^2}}\right] \tag{15}$$

$$L_{lwr} = \left[b_0 + b_1 t_{s,lwr} \pm t_{95,n-2}\, s\sqrt{\frac{1}{n} + \frac{(t_{s,lwr} - \bar{x})^2}{\sum_{i=1}^{n}(x_i - \bar{x})^2}}\right] \tag{16}$$

Equations (15) and (16) have four solutions. For better readability, we define the sum of squares as $SS \equiv \sum_{i=1}^{n}(x_i - \bar{x})^2$. Solution 1 of eq. (15) is

$$t_{s,upr} = -\frac{b_1\left(b_0 - L_{upr}\right)SS + s^2 t_{95,n-2}\bar{x} + s t_{95,n-2}\sqrt{\frac{1}{n}SS\left(b_1^2 SS - s^2 t_{95,n-2}^2 + n(b_0 - L_{upr} + b_1\bar{x})\right)}}{b_1^2 SS - s^2 t_{95,n-2}} \tag{17}$$

and solution 2 is

$$t_{s,upr} = \frac{b_1\left(L_{upr} - b_0\right)SS - s^2 t_{95,n-2}\bar{x} + s t_{95,n-2}\sqrt{\frac{1}{n}SS\left(b_1^2 SS - s^2 t_{95,n-2}^2 + n(b_0 - L_{upr} + b_1\bar{x})\right)}}{b_1^2 SS - s^2 t_{95,n-2}} \tag{18}$$

Solutions 3 and 4 for solving eq. (16) for $t_{s,lwr}$ are obtained by replacing L_{upr} with L_{lwr} in solutions 1 and 2, respectively. For the present study, we found that solution 1 provides estimates for t_{upr} of 10.85 years (D), 6.07 years (σ), 12.0 years (N) and 14.96 years (c). A summary of the parameters from the long-term stability study is given in Table 5. The same principle as for estimation of the shelf-life may be used for choosing an initial monitoring point for post-certification monitoring of stability. To determine appropriate post certification monitoring points, we consider the rates of the change of the measurand values. Assuming a linear trend, the rates per year are b_1= -0.01 nm for D, 0.02 nm for σ, 0.04 $\times$ 10^{-6} mol l^{-1} for N and 0.04 g l^{-1} for c . The measurements show clear differences in the individual parameters. It would therefore be very interesting to understand where these differences come from. However, such research would take further years and is therefore outside the scope of the current study. Therefore, we limit ourselves at this point to stating the fact that the yearly changes are acceptable with respect to the defined target uncertainties. To control the possible further change of the measurand parameters, we set one monitoring point per year. This ensures that any future change of the parameter values that may take place will be detected. For estimation of the stability uncertainties in the absence of significant

trends, we employ clause 8.7.3 of ISO Guide 35[2] and use

$$u_{lts} = \sqrt{u_{lts,1}^2 + u_{lts,2}^2} \tag{19}$$

with

$$u_{lts,1} = s(b_1)(t_{m1} + t_{cert}) \tag{20}$$

(see eq. (10) at page 44 of ISO Guide 35) and

$$u_{lts,2} = \frac{b_1}{2\sqrt{3}} t_{cert} \tag{21}$$

under the assumption of an equal distribution of the values (rectangular function). The t_{m1} is the time interval between value assignment and the initial stability monitoring point (rounded up to 5 years) and t_{cert} is the planned lifetime (here 5 years). The correspondingly estimated uncertainty contributions u_{lts}, ranging between 1.43% and 4.65% of the mean values of the measurands are provided in Table 7).

Table 5: Parameters of the long-term stability study. y_m is the mean value of a measurand and s is its standard deviation, u_t is the target uncertainty, given in units of the measurand and in % of y_m, b_0 is the regression parameter (eq. 7) and s_{b0} is its standard error (eq. (10), b_1 is the slope of the regression (eq. 6) and s_{b1} is its standard error (eq. (8)), t_{b1} is the t-statistic of b_1 (eq. (11)), $t_{95,n-2}$ is the two-tailed critical value for Student's t and t_{shelf} it the predicted shelf life in years, u_{lts} is the uncertainty contribution caused by instability in units of the measurand and in % of y_m.

Measurand	y_m	s	u_t	b_0	s_{b0}	b_1	s_{b1}	t_{b1}	$t_{95,n-2}$	t_{shelf}	u_{lts}
D (nm)	5.82	0.14	0.29 (5%)	5.83	0.02	-0.01	0.01	1.15	1.99	10.85	0.13 (2.26%)
σ (nm)	1.34	0.05	0.13 (10%)	1.33	0.01	0.02	0.0	5.86	1.99	6.07	0.05 (3.47%)
N (10^{-6}mol /l)	3.77	0.19	0.76 (20%)	3.73	0.02	0.04	0.01	3.5	1.99	12.0	0.18 (4.65%)
c (g/l)	3.07	0.05	0.62 (20%)	3.04	0.01	0.04	0.0	12.16	1.99	14.96	0.04 (1.43%)

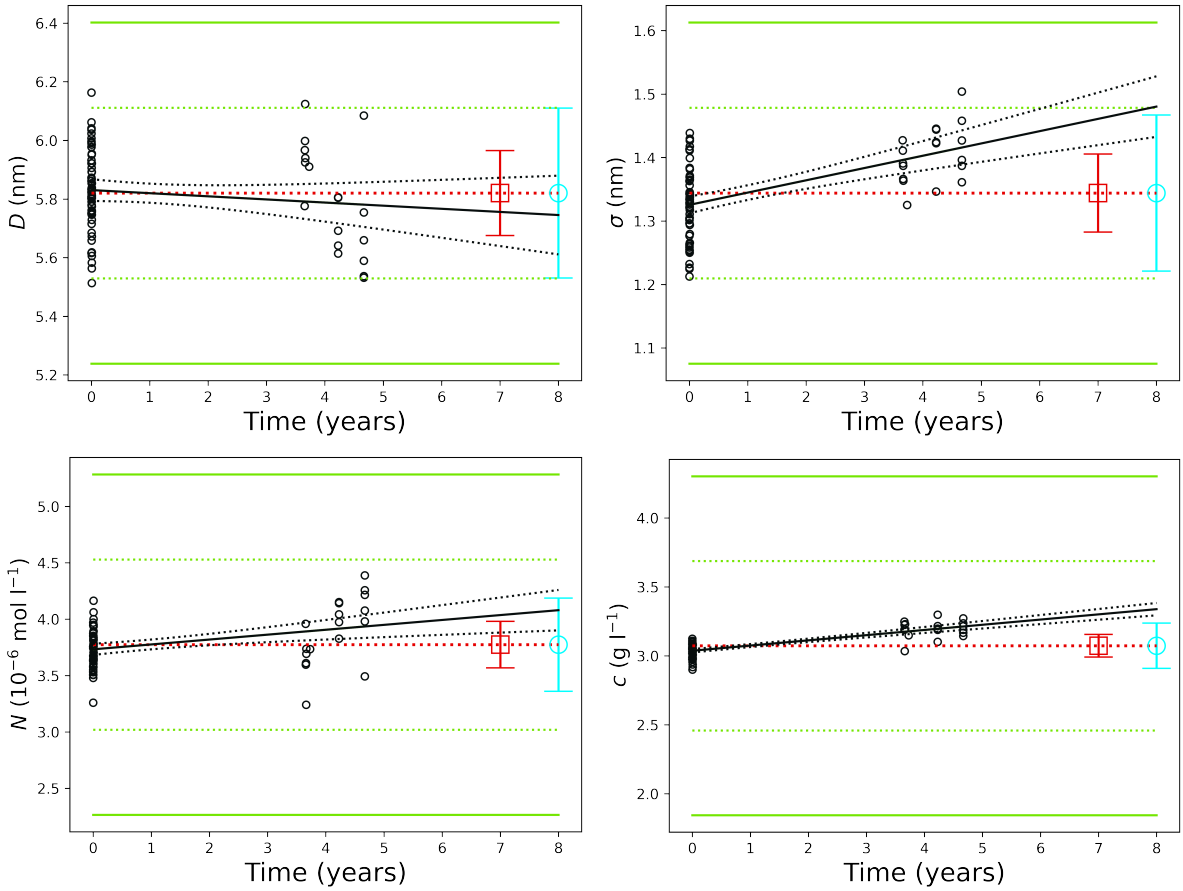

Figure 4: Long-term stability study on the diameter D, diameter distribution width σ, particle number density N and particle concentration c. Given are measurand values (black circles), mean of the values (dotted red line), one and two standard deviations of the mean values (red and blue error bars, respectively), linear regression lines (black solid lines) and their 95% level of confidence (area between dashed black lines). One and two standard deviations of the target uncertainties are shown as horizontal dashed and solid green lines.

5 Characterization

5.1 Analytical Methods

The certification of the silver nanomaterial is based on the SAXS instrumentation and the SAXS method, which has been validated and for which the total measurement uncertainty is available [17, 18, 19]. SAXS is an established method for metrologically traceable determination of the diameter of spherical particles and does not require sample preparation or calibration [17]. In the round-up to this reference material development, we conducted an international SAXS interlaboratory comparison as a feasibility study [20]. The material of that study was a suspension of silver nanoparticles, prepared in the same way as BAM-N008. The measurand values for D, σ, N and c of that study were reliably determined. Therefore, we were guided here by the outcome of this interlaboratory comparison for the choice of the measurands. Small-angle X-ray scattering was used throughout for homogeneity and stability testing as well as the characterization of the material. For material characterization, three independent reference instruments were employed. The first instrument used at the BAM laboratories is a SAXSess (Anton Paar AG, Austria). This Kratky type of instrument is attached to a laboratory X-ray generator (PW3830, PANalytical), and was operated with a fine focus glass X-ray tube at 40 kV and 40 mA (CuK$_\alpha$, λ=0.1542 nm). A focusing multi-layer optic and a block collimator provide a monochromatic primary beam with low background, as reported by Bergmann et al. [21]. Samples with a volume of 50 μl were filled in a flow through plastic capillary with an inner diameter of 1 mm. The flow through capillary allows to attain the same scattering volume for the scattering of i.) sample, ii.) solvent and iii.) empty capillary. The scattered intensity as function of the scattering vector q was recorded with a Mythen detection system (Dectris AG, Switzerland). The intensity data were converted to absolute intensity data with SAXSquant software (Anton Paar AG) as described by Orthaber et al. [22]. Data were taken for a q-range between 0.1 nm^{-1} and 3 nm^{-1}. Data outside this range were discarded. The temperature was controlled with a TCS 120 sample holder (Anton Paar AG) with an accuracy of ±1°C. The scattering curves measured for the homogeneity study is displayed in Figure 5. The second instrument used at the BAM laboratories was a Nano-inXider (Xenocs, Grenoble, France). The third instrument was the SAXS setup of the Physikalisch Technische Bundesanstalt (PTB, Berlin, Germany). This instrument is located at the laboratories of the Helmholtz-Zentrum Berlin für Materialien und Energie (HZB), installed at the PTB four-crystal monochromator beam line [19]. The sample to be studied was injected in a glass capillary with an inner diameter of 1 mm and a wall thickness of 10 µm. Scattering patterns were registered for a measuring time of 3600 s with a CCD-based detector at a photon energy of 10 keV. The sample to detector distance was 2.561 m. The transmitted beam through the sample was blocked by a rectangular beam stop in front of the detector. The scattering pattern obtained from a capillary filled with water was used to correct for background contributions. The intensity values from instrument 3 were not scaled to absolute intensities.

The SAXS data were evaluated according to the international standard ISO 17867 [1] employing the model of a lognormal size distribution of spherical particles. Application of this model is exemplarily shown in Figure 6 for a data set from a measurement taken in the homogeneity study (measurement identifier is S9602, sample ID is 970). The curve fits provide estimated of the distributions of the silver nanoparticle diameters, which are shown in Figure 7. A detailed explanation on the data evaluation is given in clause 5.2.

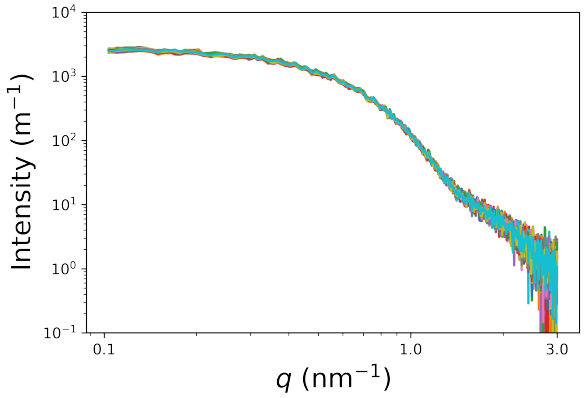

Figure 5: Overlay of 60 SAXS data sets of the homogeneity stability study. The scattering intensity is given in absolute units of [Intensity] = m^{-1} using water for absolute calibration according to Orthaber et al. [22].

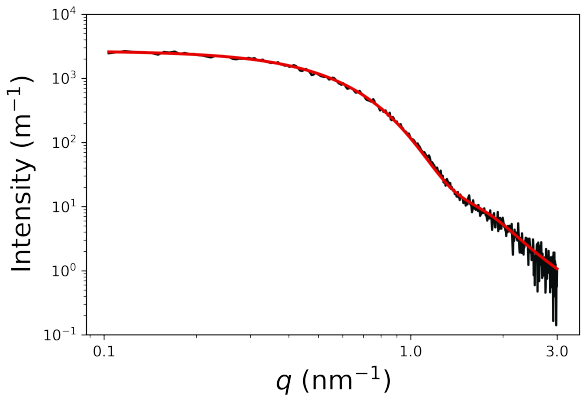

Figure 6: Interpretation of the SAXS data by application of the model according to eq. (22). Given is the scattering data in terms of the scattering intensity as a function of the scattering vector q and the best fit of the model (black and red solid line, respectively). The data set S9602 from the sample with the ID 970 is from the homogeneity study. Data in the q-range between 0.1 nm^{-1} and 3.0 nm^{-1} were chosen for data evaluation. Data outside this range were discarded.

The minimum sample intake for a measurement for determination of the particle properties should be chosen in a way that no significant heterogeneity within the sample is to be expected. For SAXS measurements, however, the sample intake is mainly determined by the size and capacity of the capillary, so no specific recommendation is given. For the instruments used in this study, considerable homogeneity has been proven, such that the dimensions of the capillary were suitable (see chapter 3). As a general recommendation, at least 50 μl of the suspension should be used for a single analysis. Although this has not been tested here, it can be assumed that using smaller

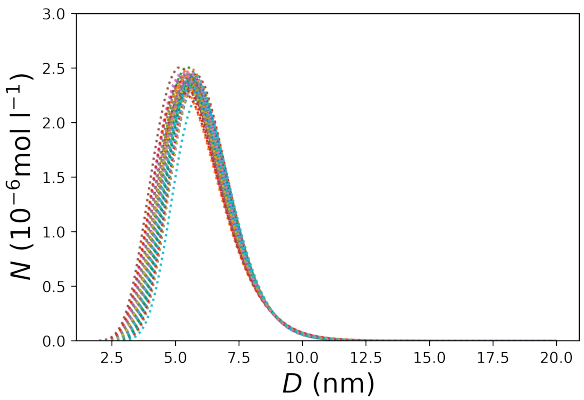

Figure 7: Overlay of 60 diameter size distributions as obtained from the SAXS data shown in Figure 5. The size distributions are number-weighted, and the distributions' shape is a lognormal function.

volumes than 50 microliters for the measurements will give the same results. This assumption is indicated by an earlier study on certified reference materials of gold nanoparticles in which only 20 and 3 μl of suspension were used [23].

5.2 Analytical results and statistical evaluation

5.2.1 Model for interpretation of the SAXS data

A model-driven small-angle X-ray scattering data evaluation was performed for characterization of the size distribution and the concentration of the silver nanoparticles. The SAXS model of non-interacting spheres was utilized in accordance with ISO 17867 [1] on the assumption of a constant internal density within the particles and that the particles are dispersed in a homogeneous continuous phase. This model is given as

$$I(q) = N_n(\rho_2 - \rho_1)^2 \int_0^\infty f(r) \left[\frac{4\pi}{3} r^3\right]^2 P(q,r)dr \tag{22}$$

where $I(q)$ is the scattering intensity, q is the scattering vector, N_n is the particle number density, ρ_2 is the scattering length density of the particles (silver) and ρ_1 is the scattering length density of the continuous phase (water). Specifically, the ρ-values were calculated with the scattering length density calculation tool of the program SASfit [24]. Calculated values were ρ_2 = 7.738×10^{11} cm^{-2} for a silver density of 10.49 g cm^{-3} and a copper K$_\alpha$-energy of 8047.60 eV. An ρ_1 = 9.446×10^{10} cm^{-2} was calculated for water with a density of 0.998 g cm^{-3}. Hence, we employed a scattering length density difference of $\rho_2 - \rho_1$ = 6.793×10^{11} cm^{-2}. The scattering vector is defined as $q = 4\pi\lambda^{-1} \sin\theta$ with the wavelength of the X-ray beam $\lambda = 0.15418$ nm and the scattering angle θ. The $f(r)$

is the particles' number-weighted radii distribution and $P(q,r)$ is their form factor with

$$P(q,r) = \left[3\frac{\sin(qr) - qr\cos(qr)}{(qr)^3}\right]^2 \tag{23}$$

In this study $f(r)$ is the lognormal distribution, which is recommended in the standard ISO 17867 [1] and was successfully employed earlier in an interlaboratory comparison for determination of particle size distribution with SAXS (see [20]). The lognormal size distribution is defined as

$$f(R) = \frac{1}{\sqrt{2\pi}\,wR}\exp\left[-\frac{\ln\left(R/R_{median}\right)^2}{2w^2}\right] \tag{24}$$

where R_{median} is the median of the radii and w defines the width of the distribution. It should be noted that w is the standard deviation of the natural logarithm of the radii distribution width (unit is 1), and must not be confused with the standard deviation of the radii distribution width itself (unit is nm). Since the shape of the lognormal distribution is defined by R_{median} and w, further parameters of interest can be derived thereof. The most frequently used derived parameters are mean, modal and standard deviation. The mean value of the radii is

$$R_{mean} = R_{median}\exp\left(w^2/2\right) \tag{25}$$

with an uncertainty of

$$u_{R_{mean}} = \left[e^{w^2}\left(u^2_{R_{median}} + \left[R_{median}w\,u_w\right]^2\right)\right]^{1/2} \tag{26}$$

where estimates of the uncertainties $u_{R_{mean}}$ and u_w were provided from the fit procedure (for details see [24]). The radii size distribution width is

$$\sigma_{lognormal} = \left[e^{2w^2} - e^{w^2}\right]^{1/2} R_{median} \tag{27}$$

with an uncertainty of

$$u_{\sigma_{lognormal}} = \left(\left[e^{2w^2} - e^{w^2}\right]u^2_{R_{median}} + \frac{e^{w^2}\left(1 - 2e^{w^2}\right)^2 R^2_{median}w^2}{e^{w^2} - 1}u^2_w\right)^{1/2} \tag{28}$$

We employ $N_{fit} = N_n(\rho_2 - \rho_1)^2$ as scaling factor to avoid a numerically unfavorable usage of very large numbers of N_n and very small numbers of $(\rho_2 - \rho_1)^2$ in the curve fitting process. Together with the abbreviation $I_{fit} = \int_0^\infty f(r)\left[\frac{4\pi}{3}r^3\right]^2 P(q,r)dr$ we obtain

$$I(q) = N_{fit}I_{fit} \tag{29}$$

where I_{fit} represents the q-dependent term of the curve fitting procedure, providing the parameters R_{median} and w. The particles' diameter was calculated utilizing eq. (25) as

$$D = 2R_{median} \tag{30}$$

with an uncertainty of

$$u_D = 2u_{R_{median}} \tag{31}$$

The size distribution width of the diameter was derived from eq. (27) as

$$\sigma = 2\sigma_{lognormal} \tag{32}$$

with an uncertainty of

$$u_\sigma = 2u_{\sigma_{lognormal}} \tag{33}$$

5.2.2 Number density of particles

The units of absolute intensity $I(q)$, scattering vector q and the scattering length densities ρ_2 and ρ_1 had to be considered to convert the scaling factor N_{fit} to a particle concentration (in number of particles per cm^3). From the model employed, we get $N_{fit} = I(q)\, I_{fit}^{-1}$. The units of the measured intensity $[I(q)] =$ m^{-1} and the fit intensity $[I_{fit}] =$ nm^6 provide $[N_{fit}] = [I]\,[I_{fit}]^{-1} =$m^{-1}nm^{-6}. The number density is given by

$$N_n = \frac{N_{fit}}{(\rho_2 - \rho_1)^2} \tag{34}$$

where the unit for the square of the scattering length density difference is $\left[(\rho_2 - \rho_1)^2\right] =$ cm^{-4}. Therefore, we get

$$[N_n] = \frac{[N_{fit}]}{[(\rho_2 - \rho_1)^2]} \tag{35}$$

$$= \frac{\text{m}^{-1}\text{nm}^{-6}}{\text{cm}^{-4}} \tag{36}$$

$$= 10^{40}\text{cm}^{-3} \tag{37}$$

This means that we have to multiply the calculated $N_{fit}/(\rho_2 - \rho_1)^2$-values by a factor of 10^{40} to obtain particle number densities N_n in units of cm^{-3}. The uncertainty of N_n depends on the uncertainties of N_{fit}, ρ_2 and ρ_1. The uncertainty of N_{fit} can be estimated as the uncertainty from the curve fit $u_{N_{fit}}$. In contrast, no reliable uncertainty estimates are available for ρ_2 and ρ_1. Therefore, the standard uncertainty, as calculated according to

GUM [25], is simply estimated as

$$u_{N_n} = \frac{u_{N_{fit}}}{(\rho_2 - \rho_1)^2} \tag{38}$$

In chemistry, molar concentrations are typically in use. Molar concentrations are obtained from particle number densities by

$$N = \frac{N_n}{N_A} \tag{39}$$

with an uncertainty of

$$u_N = \frac{u_{N_n}}{N_A} \tag{40}$$

The N_A is the Avogadro number defined as $N_A = 6.02214076 \times 10^{23}$ mol^{-1}. The units are

$$[N] = \frac{[N_n]}{[N_A]} \tag{41}$$

$$= \text{mol cm}^{-3} \tag{42}$$

$$= 10^6 \text{ mol l}^{-3} \tag{43}$$

Therefore, the values of N_n and u_{N_n} have to be multiplied by $10^6 N_A$ for conversion of number densities in units of cm^{-3} to molar concentration in units of mol l^{-1}.

5.2.3 Weight concentration

The particle concentration c in units of $[c] =$ g cm^{-3} is given by

$$c = N_n \rho \langle V \rangle \tag{44}$$

where N_n is the particle number density, ρ is the density of the particles and $\langle V \rangle$ is the mean particle volume. Uncertainties can be estimated for N_n and $\langle V \rangle$ from the curve fit parameters. No uncertainty is available for ρ, the density of silver nanoparticles. Here the density of silver as bulk material of 10.49 g cm^{-3} was employed. The combined standard uncertainty, as calculated according to GUM [25] is

$$u_{\text{con}} = \sqrt{u_1^2 + u_2^2} \tag{45}$$

The first contribution to u_{con} depends on the uncertainty of N_n and is

$$u_1 = \rho \langle V \rangle u_{N_n} \tag{46}$$

The second contribution to u_{con} is

$$u_2 = N_n \rho u_{\langle V \rangle} \tag{47}$$

and depends on the uncertainty of $\langle V \rangle$, which in turn depends on the particle size distribution. For spherical particles apply

$$\langle V \rangle = 4/3\pi \left\langle R^3 \right\rangle \tag{48}$$

and the radii distribution needs to be taken into account for correct calculation of $\langle V \rangle$. The mean volume of particles with a lognormal radii distribution is

$$\langle V \rangle = \frac{4\pi}{3} R^3_{median} \exp\left[\frac{9w^2}{2}\right] \tag{49}$$

Its combined standard uncertainty is

$$u_{\langle V \rangle} = \sqrt{u_{21}^2 + u_{22}^2} \tag{50}$$

with

$$u_{21}^2 = \left(4\pi R^2_{median} \exp\left[\frac{9w^2}{2}\right]\right)^2 u^2_{R_{median}} \tag{51}$$

$$u_{22}^2 = \left(12\pi w R^3_{median} \exp\left[\frac{9w^2}{2}\right]\right)^2 u_w^2 \tag{52}$$

5.2.4 Instrument related bias

The homogeneity, short-term and long-term stability studies were performed with the same SAXS instrument as described in the experimental section. It is a slit-focus Kratky-type of instrument, which has been introduced in its present form in 2000 [21]. This instrument has been proven to be particularly suitable for measurements of nanoparticles in solution because of a short sample-to-detector distance. The slit-focus geometry in combination with a low sample-to-detectors distance allows precise measurements of the scattering intensity of water as secondary standard for determination of the absolute intensity [22]. Reliable absolute intensity values in turn are important for determining reliable particle number densities and particle mass concentrations. Furthermore, for proficiency testing, exactly this instrument was employed in an interlaboratory comparison for silver nanopar-

ticles size distribution quantification [20]. Therefore, instrument 1 appears suitable for the nanoparticle reference material development. Nevertheless, the possibility of an experimental bias must be ruled out. For this purpose, measurements of the silver nanomaterial were carried out on two further SAXS instruments, allowing to identify possible sources of instrument-related bias of the measurements. For maximizing possible effects of experimental bias, the two additionally selected instruments were chosen of highly different construction compared to instrument one. Instrument two was a pinhole lab-instrument operating with a vertical x-ray beam. This commercial instrument has been reported to allow robust and traceable measurements of number concentrations for gold nanoparticles [26]. Instrument three is non-commercial, operates with synchrotron radiation and is regularly employed for metrological studies [17, 18]. Measurements with instrument two were carried out according to the manufacturer's protocol and instrument three according to the procedure of PTB, the metrological institute of Germany [19]. Ten randomly selected samples were measured with instrument two and the resultant data were evaluated in the same way as for the data from instrument one. The overall means of the results from data from instrument two are D = (5.94 ± 0.16) nm, σ = (1.32 ± 0.05) nm, N = (3.85 ± 0.28) $\times$ 10^{-6} mol/l and c = (3.27 ± 0.07) g l^{-1}. Two randomly selected samples were measured with instrument three by PTB. Data evaluation provides 6.25 nm and 5.86 nm for D and 1.37 nm and 1.28 nm for σ. Here, the N and c could not be determined because the intensity values were not on an absolute scale. The results obtained with instruments two and three are in agreement with the results of the homogeneity study obtained with instrument one. This finding suggests that there is little or no influence on the use of a specific SAXS instrument. The mentioned interlaboratory comparison on silver nanoparticles also confirms this assumption [20].

6 Property values and their uncertainties

6.1 Assigned measurand values

The assigned value of each of the measurands (y_{char}) is calculated as the arithmetic mean

$$y_{\text{char}} = \frac{1}{60}\sum_{i=1}^{60} y_i \tag{53}$$

of 60 data sets (y_i) from the homogeneity study (see clause 3) providing D = 5.83 nm, σ = 1.33 nm, N = 3.74 × 10^{-6} mol l^{-1} and c = 3.04 g l^{-1}. An overview of the measurand values is provided in Figure 8 as box and whisker plots. Red squares represent the mean values of the measurands (red squares). Red solid lines correspond to the assigned measurand values. Ranges for assigned values with ±1 and ±2 times the target uncertainty of 5% (D), 10% (σ), 20% (N), 20% (c) are indicated (dashed and solid green lines, respectively). It can be clearly seen that the whiskers for the values are within two standard deviations of the target uncertainties. Therefore, the data were considered as reasonably justified. Boxes in Figure 8 represent the interquartile ranges between Q_1 = 25% and Q_3 = 75%. Whiskers are set to 5% and 95%. Data beyond the whiskers are marked as individual points.

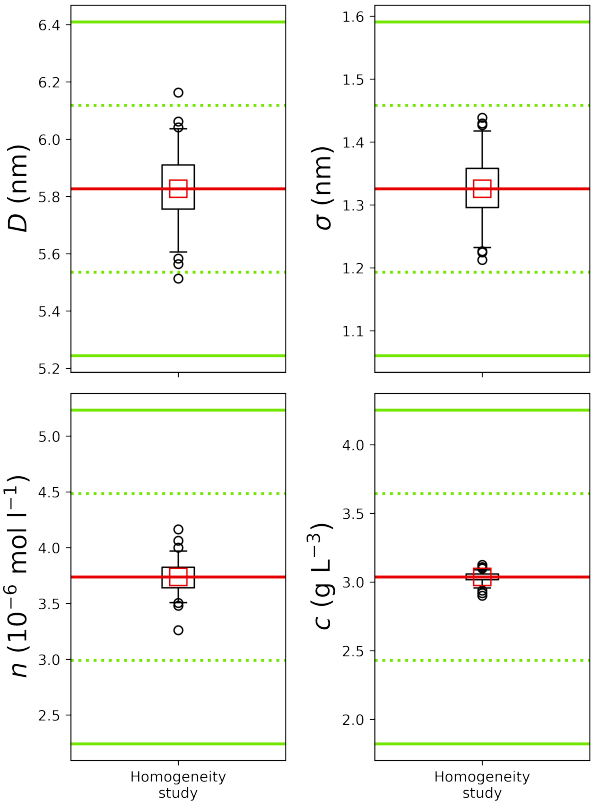

Figure 8: Assigned measurand values as determined from the homogeneity study are D = 5.83 nm, σ = 1.33 nm, N = 3.74 × 10^{-6} mol l^{-1} and c = 3.04 g l^{-1}. Boxes represent the interquartile ranges between Q_1 = 25% and Q_3 = 75%. Whiskers are set to 5% and 95%. Data beyond the whiskers are marked as individual points. The targeted range of assigned values with ±1 and ±2 times the targeted uncertainty of 5% (D), 10% (σ), 20% (N), 20% (c) are indicated (dashed and solid green lines, respectively).

6.2 Uncertainty evaluation

Different sources of uncertainty contribute to the uncertainty of each measurand and were taken into account. The sources of uncertainties (homogeneity, repeatability, stability and bias) and the way of calculating the corresponding contributions are listed and explained in Table 6. The uncertainty estimates (u_{bb}, u_{rep}, u_{lts} and u_{bias}) have been derived from the experiments as described above and displayed in Figure 9. It can be seen that u_{bb} is the smallest and u_{lts} is the largest contribution. This finding can be considered typical for nanoparticles in dispersion originating from a uniform batch. The high Brownian motion of the nanoparticles ensures a homogeneous mixture of the batch. On the other hand, the Brownian motion of the sub-10 nm particles ensures a high collision rate with each other and the walls of the bottles, producing the danger of aggregation and deposition on the wall. The relative uncertainties of the measurands are plotted in Figure 10 for a better overview. The combined uncertainties were calculated as

$$u_c = \left(u_{bb}^2 + u_{rep}^2 + u_{lts}^2 + u_{bias}^2\right)^{1/2} \tag{54}$$

Application of eq. (54) provides u_c-values of 3.8% (D), 7.1% (σ), 11.3% (N) and 12.3% (c), which are all substantially below the respective target values of 5%, 10%, 20% and 20% (see Table 7 and Figure 10). The expanded uncertainties, calculated as $U = k \times u_c$ with an expansion factor of k=2, are also provided in Table 7. These U-values are part of the BAM-N008 certificate.

Table 6: Uncertainty contributions and their estimation.

Source	Symbol	Meaning and estimation
Homogeneity	u_{bb}	Homogeneity contribution from the homogeneity study as described in chapter 3
Repeatability	u_{rep}	Repeatability of a single measurement derived from the ANOVA analysis as the average repeatability of the full set of measurements (see chapter 3)
Stability	u_{lts}	Estimate of a contribution due to possible changes of the measurands derived from the long-term stability study as described in chapter 4.2
Bias	u_{bias}	The greater of $u_{bias,1}$ and $u_{bias,2}$. $u_{bias,1}$ is the difference of the comparison with the gold standard reference material SRM 8011 (see section 7). $u_{bias,2}$ is the difference of the comparison with instrument two (see section 5.2.4).

Table 7: Values of the uncertainty contributions, combined uncertainties, and expanded uncertainties.

Parameter (Unit)	Diameter D (nm)	Size distribution width σ (nm)	Number density N (10^{-6}mol l^{-1})	Concentration c (g cm^{-3})
Value	5.8	1.33	3.7	3.0
Uncertainty contributions				
Homogeneity, u_{bb}	0.03 (0.6%)	0.00 (0.0%)	0.05 (1.4%)	0.00 (0.0%)
Repeatability, u_{rep}	0.13 (2.2%)	0.05 (4.0%)	0.15 (3.9%)	0.04 (1.5%)
Stability u_{lts}	0.14 (2.5%)	0.06 (4.6%)	0.21 (5.5%)	0.08 (2.7%)
Bias, u_{bias}	0.11 (1.9%)	0.03 (2.4%)	0.23 (6.1%)	0.24 (7.8%)
Combined uncertainties				
u_c	0.22 (3.9%)	0.09 (6.6%)	0.34 (9.2%)	0.25 (8.3%)
Expanded uncertainties				
U	0.5 (9%)	0.18 (14%)	0.7 (19%)	0.5 (17%)

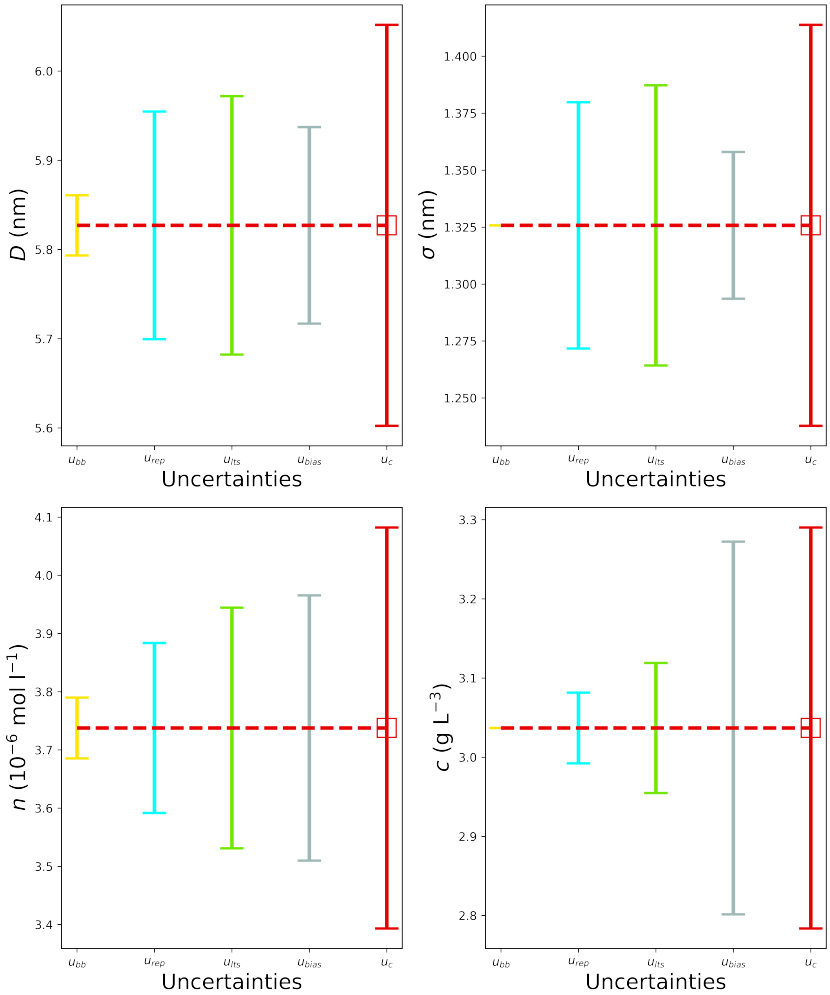

Figure 9: Uncertainty contributions (u_{bb}, u_{rep}, u_{lts}, u_{bias}) and the combined uncertainties u_c for diameter D, size distribution width σ, number density N and concentration c.

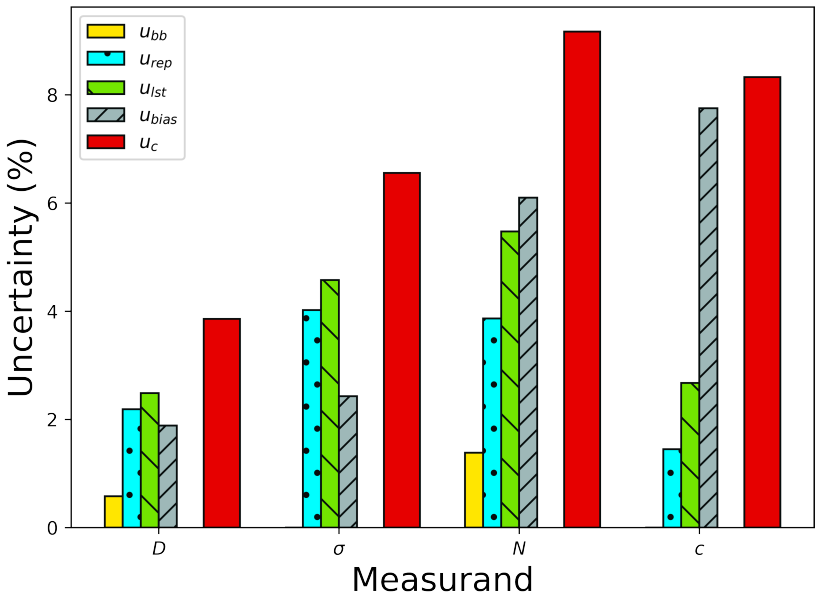

Figure 10: Overview on the relative uncertainty contributions ($u_{bb}, u_{rep}, u_{lts}, u_{bias}$) and the combined uncertainties u_c of diameter D, size distribution width σ, number density N and concentration c.

7 Metrological traceability

The four measurands under consideration in this study are from theory all traceable to SI units. But in this work, traceability will be limited to particle diameter. Direct traceability of the diameter can be established to SRM 8011, which is a certified reference material from NIST consisting of gold nanoparticles in water [27]. Its certified diameter is D_{RM8011} = (8.5 ± 0.4) nm. Data on the size distribution width of SRM 8011 is available from literature [23]. The reported polydispersity value of 7% allows an estimate of the size distribution width of σ_{RM8011} = (0.6 ± 0.2) nm. But traceability has not been proven for σ_{RM8011}, N and c.

Five samples of RM 8011 were measured with instrument one using the same measurement conditions and followed by the same model data evaluation as applied for the silver nanomaterial. The resulting model curve fits provide estimates of D, σ, N and c. An overview of the parameter values is provided in Figure 11. A performance statistics was applied for comparison with the reference values in terms of normalized errors (En-values) according to ISO 17043 [28]. The normalized errors were calculated as

$$E_n = \frac{x - X}{\sqrt{U_{lab}^2 + U_{ref}^2}} \tag{55}$$

The x is the measured result, X is the assigned value, U_{lab} is the combined expanded uncertainty of a measured result and U_{ref} is the combined expanded uncertainty of the reference value. A normalized error of $|E_n| \leq 1.0$ indicates "satisfactory" performance while $|E_n| > 1.0$ indicates "unsatisfactory" performance. The results of the single measurements of NIST SRM 8011 provide $|E_n|$-values in the range of 0.07 to 0.36, i.e., they are well below 1 for all measurands which proofs that measured and certified values are fully consistent (see Table 8). This indicates a "satisfactory" performance and the absence of outliers. Next, the measured values were pooled, and the resultant experimental mean values of the measurands were compared with the reference values as also shown in Table 8. The results for RM 8011 provide a contribution to the uncertainty of the measurands of the silver nanoparticles in the form of a remaining bias, $u_{bias,1}$. The $u_{bias,1}$ is estimated as the difference between the reference values and measured values. As can be seen in Table 8, the relative values of $u_{bias,1}$ is 0.9% for D. These relative $u_{bias,1}$-value is included in the total uncertainty budget. The above calibration against the NIST reference material SRM 8011 confirms the correctness of the SAXS measurements from which the D, s, N and c were calculated using the physical model of non-interacting homogeneous spheres. Given the above, it is reasonable to conclude that the values for the parameter D of BAM-N008 is traceable to the SI under the assumptions of the model used.

Table 8: Parameters determined experimentally for gold standard reference material SRM 8011 in comparison with the reference values. Normalized errors (E_n-values) of < 1 proof "satisfactory" performances. Difference between reference values and measured values are listed as bias-values $u_{\text{bias},1}$, i.e., the uncertainty contributions due to evaluation with SRM 8011.

Property	Unit	Reference Value	Measured Value	Difference	E_n	$u_{\text{bias},1}(\%)$
D	nm	$8.50\times10^{0} \pm 4.00\times10^{-1}$	$8.66\times10^{0} \pm 3.41\times10^{-3}$	0.16 (1.93%)	0.21	0.967
σ	nm	$6.00\times10^{-1} \pm 2.00\times10^{-1}$	$6.29\times10^{-1} \pm 3.54\times10^{-4}$	0.029 (4.86%)	0.073	2.43
N	cm^{-3}	$7.08\times10^{+12} \pm 1.13\times10^{+12}$	$7.94\times10^{+12} \pm 1.20\times10^{+10}$	$8.6\times10^{+11}$ (12.21%)	0.38	6.1
c	g l^{-1}	$5.16\times10^{-5} \pm 2.64\times10^{-6}$	$5.35\times10^{-5} \pm 8.00\times10^{-8}$	1.9×10^{-6} (3.74%)	0.36	1.87

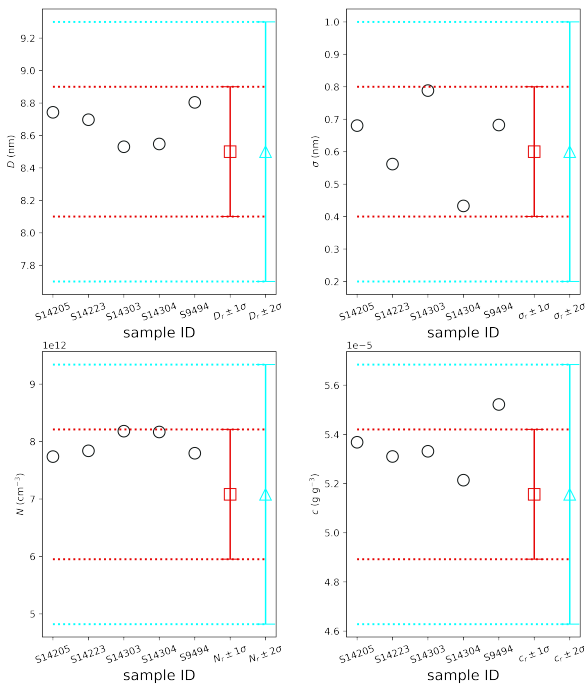

Figure 11: Measured parameters for the gold standard reference material SRM 8011 (black circles). The reference values for D, σ, N and c are provided with uncertainties of one and two standard deviations (red and blue error bars).

8 Information on the proper use of the RM

8.1 Recommended use

The intended purpose of BAM-N008 is the verification of analytical results obtained for determination of diameter, size distribution width, number density and mass concentration of nanoparticles in dispersion. Preferably, for quality control of particle size analysis with the SAXS method according to ISO 17867 [1]. In addition, this reference material should open also the possibility to study technical processes like catalysis or biomedical processes directly in living objects [29, 30, 31].

8.2 Transport, storage and handling

BAM-N008 can be shipped at ambient temperature. Upon receipt, the material should be stored in the dark at a temperature of (20±3) °C in its original tightly closed bottle. When handling the sample, the bottle shall be left unclosed as short as possible. BAM cannot be held responsible for changes that happen during storage of the material at the customer's premises, especially of opened samples. The material should be used as it is from the bottle. However, before taking a sample, homogenization by manually shaking the closed bottle for 20 seconds is strongly recommended.

8.3 Shelf-life

The initial stability study after storage of selected units indicate an increase of the certified properties. Therefore, starting with dispatch of the material from BAM, the validity of the certificate expires after 12 months. Post-certification measurements will be conducted in appropriate periods to keep this information up to date.

8.4 Safety information

The usual laboratory safety precautions for handling liquids have to be applied. No hazardous effects are to be expected when the material is used under conditions commonly adopted for the analysis of samples containing aqueous dispersions of nanoparticles. It is strongly recommended handling and disposing the reference material in accordance with the guidelines for hazardous materials legally in force at the site of end use and disposal.

8.5 Legal notice

Neither BAM, its contractors nor any person acting on their behalf:

(a.) make any warranty or representation, express or implied, that the use of any information, material, apparatus, method or process disclosed in this document does not infringe any privately owned intellectual property rights; or

(b.) assume any liability with respect to, or for damages resulting from, the use of any information, material, apparatus, method or process disclosed in this document.

9 Information on and purchase of the RM

The reference material BAM-N008 is supplied by

Bundesanstalt für Materialforschung und -prüfung (BAM)

Unter den Eichen 87

12205 Berlin, Germany

Orders can be placed at www.webshop.bam.de

Each sample of BAM-N008 will be distributed together with a detailed certificate containing the parameter values and their uncertainties, the mean values and standard deviations of all accepted data sets and information on the analytical methods used.

Information on BAM reference materials are available from BAM at https://www.bam.de.

10 References

[1] International Organization for Standardization. "Particle size analysis - Small-angle X-ray scattering (SAXS)". ISO 17867:2020(E).

[2] International Organization for Standardization. "Reference materials – Guidance for characterization and assessment of homogeneity and stability". ISO Guide 35:2017(E).

[3] J. Zhu et al. "Recent Advances in Electrocatalytic Hydrogen Evolution Using Nanoparticles". Chemical Reviews 120 (2020), pp. 851–918. DOI: 10.1021/acs.chemrev.9b00248.

[4] E. Valsami-Jones and I. Lynch. "How safe are nanomaterials?" Science 350 (2015), pp. 388–389. DOI: 10.1126/science.aad0768.

[5] S. Eckhardt et al. "Nanobio Silver: Its Interactions with Peptides and Bacteria, and Its Uses in Medicine". Chemical Reviews 113 (2013), pp. 4708–4754. DOI: 10.1021/cr300288v.

[6] S. Chernousova and M. Epple. "Silver as antibacterial agent: ion, nanoparticle, and metal". Angewandte Chemie (International ed. in English) 52 (2013), pp. 1636–53. DOI: 10.1002/anie.201205923.

[7] N. Duran, W. J. Favaro, and A. B. Seabra. "What do we Really Know about Nanotoxicology of Silver Nanoparticles In vivo? New Aspects, Possible Mechanisms, and Perspectives". Current Nanoscience 17 (2021), pp. 292–320. DOI: 10.2174/1573413714666180809121322.

[8] Z. Ferdous and A. Nemmar. "Health Impact of Silver Nanoparticles: A Review of the Biodistribution and Toxicity Following Various Routes of Exposure". International Journal of Molecular Sciences 21 (2020). DOI: 10.3390/ijms21072375.

[9] L. Li et al. "Controllable synthesis of monodispersed silver nanoparticles as standards for quantitative assessment of their cytotoxicity". Biomaterials 33 (2012), pp. 1714–1721. DOI: 10.1016/j.biomaterials.2011.11.030.

[10] D. Hristozov et al. "Frameworks and tools for risk assessment of manufactured nanomaterials". Environment International 95 (2016), pp. 36–53. DOI: 10.1016/j.envint.2016.07.016.

[11] R. Peters et al. "Benchmarking the ACEnano Toolbox for Characterisation of Nanoparticle Size and Concentration by Interlaboratory Comparisons". en. Molecules 26 (2021), p. 5315. DOI: 10.3390/molecules26175315.

[12] A. B. Stefaniak et al. "Nanoscale reference materials for environmental, health and safety measurements: needs, gaps and opportunities". Nanotoxicology 7 (2013), pp. 1325–1337. DOI: 10.3109/17435390.2012.739664.

[13] International Organization for Standardization. "Reference Materials - General guidance for the value assignment of property values". ISO Guide 35.1 (2013).

[14] International Organization for Standardization. "Reference materials – Contents of certificates, labels and accompanying documentation". ISO Guide 31(2015), 2015, pp. 1–10.

[15] Y. X. Hu et al. "Size-controlled synthesis of highly water-soluble silver nanocrystals". Journal of Solid State Chemistry 7 (2008), pp. 1524–1529. DOI: 10.1016/j.jssc.2008.02.028.

[16] Claudia Kästner and Andreas F. Thünemann. "Catalytic Reduction of 4-Nitrophenol Using Silver Nanoparticles with Adjustable Activity". Langmuir : the ACS journal of surfaces and colloids 32 (2016), pp. 7383–91. DOI: 10.1021/acs.langmuir.6b01477.

[17] G. Gleber et al. "Traceable size determination of PMMA nanoparticles based on Small-Angle X-ray Scattering (SAXS)". Journal of Physics: Conference Series 247 (2010), p. 012027.

[18] F. Meli et al. "Traceable size determination of nanoparticles, a comparison among European metrology institutes". English. Measurement Science & Technology 23.12 (Dec. 2012), p. 125005. DOI: 10.1088/0957-0233/23/12/125005.

[19] A. Schavkan et al. "Number Concentration of Gold Nanoparticles in Suspension: SAXS and spICPMS as Traceable Methods Compared to Laboratory Methods". English. Nanomaterials 9 (Apr. 2019), p. 20. DOI: 10.3390/nano9040502.

[20] Brian R. Pauw, Claudia Kästner, and Andreas F. Thünemann. "Nanoparticle size distribution quantification: results of a small-angle X-ray scattering inter-laboratory comparison". Journal of Applied Crystallography 50 (2017), pp. 1280–1288. DOI: 10.1107/S160057671701010X.

[21] A. Bergmann et al. "Improvement of SAXS measurements on Kratky slit systems by Gobel mirrors and imaging-plate detectors". English. Journal of Applied Crystallography 33.2 (June 2000), pp. 869–875. DOI: 10.1107/s0021889800000881.

[22] D. Orthaber, A. Bergmann, and O. Glatter. "SAXS experiments on absolute scale with Kratky systems using water as a secondary standard". English. Journal of Applied Crystallography 33 (Apr. 2000), pp. 218–225. DOI: 10.1107/s0021889899015216.

[23] R. Bienert, F. Emmerling, and A. F. Thunemann. "The size distribution of 'gold standard' nanoparticles". English. Analytical and Bioanalytical Chemistry 395 (2009), pp. 1651–1660. DOI: 10.1007/s00216-009-3049-5.

[24] I. Bressler, J. Kohlbrecher, and A. F. Thünemann. "SASfit: a tool for small-angle scattering data analysis using a library of analytical expressions". English. Journal of Applied Crystallography 48 (2015), pp. 1587–1598. DOI: 10.1107/S1600576715016544.

[25] Bureau International des Poids et Measures (BIPM). "Evaluation of measurement data - Guide to the expression of uncertainty in measurement (GUM)". JCGM 100:2008(E).

[26] Xenocs. "White paper: SAXS for pharmaceutical applications" (2020).

[27] Debra L. Kaiser and Robert L. Watters. Report of Investigation, Reference Material 8011, Gold Nanoparticles, Nominal 10 nm Diameter. Tech. rep. Gaithersburg: National Institute of Standards & Technology, 2007.

[28] International Organization for Standardization. ISO/IEC 17043: Conformity Assessment – General Requirement for Proficiency Testing. ISO/IEC 17043:2010(E).

[29] A. Haase et al. "Effects of Silver Nanoparticles on Primary Mixed Neural Cell Cultures: Uptake, Oxidative Stress and Acute Calcium Responses". Toxicological Sciences 126.2 (2012), pp. 457–468. ISSN: 1096-6080. DOI: 10.1093/toxsci/kfs003. URL: %3CGo%20to%20ISI%3E://WOS:000302008600016.

[30] Axel Oberemm et al. "Proteomic responses of human intestinal Caco-2 cells exposed to silver nanoparticles and ionic silver". Journal of applied toxicology : JAT 36.3 (2016), pp. 404–13. ISSN: 1099-1263. DOI: 10.1002/jat.3231. URL: %3CGo%20to%20ISI%3E://MEDLINE:26434666.

[31] Claudia Kästner et al. "Fate of Fluorescence Labels—Their Adsorption and Desorption Kinetics to Silver Nanoparticles". Langmuir 34.24 (2018), pp. 7153–7160. ISSN: 0743-7463. DOI: 10.1021/acs.langmuir.8b01305. URL: https://doi.org/10.1021/acs.langmuir.8b01305.

11 Annexes

11.1 Information on the software used

Data processing and analysis was implemented and run with programming language Python in version 3.8.5 for 64 bit on Windows 10 (available at the website https://www.python.org). The Python modules SciPy (version 1.6.3, https://scipy.org), NumPy (1.19.2, https://numpy.org), pandas (1.1.3, https://pandas.pydata.org), Matplotlib (3.4.3, https://matplotlib.org) were used for calculations. JupyterLab (Version 2.2.6, https://jupyter.org) was used as user interface. The document was produced with LaTeX using Overleaf as a LaTeX editor (see https://overleaf.com).